



NIH Public Access

Author Manuscript

Biochemistry. Author manuscript; available in PMC 2013 September 25.

Published in final edited form as:
Biochemistry. 2012 September 25; 51(38): 7596–7607. doi:10.1021/bi300654v.

Binding by the Hepatitis C Virus NS3 Helicase Partially Melts Duplex DNA

Veronica M. Raney^{1,\$}, Kimberly A. Reynolds¹, Melody K. Harrison^{1,§}, David K. Harrison¹, Craig E. Cameron², and Kevin D. Raney^{1,*}

¹Department of Biochemistry and Molecular Biology, University of Arkansas for Medical Sciences, Little Rock, AR, 72205

²The Pennsylvania State University, University Park, PA

Abstract

Binding of NS3 helicase to DNA was investigated by footprinting with KMnO₄, which reacts preferentially with thymidine residues in ssDNA compared to those in dsDNA. A distinct pattern of reactivity was observed on ssDNA, which repeated every 8 nt and is consistent with the known binding site size of NS3. Binding to a DNA substrate containing a partial duplex was also investigated. The DNA contained a 15 nt overhang made entirely of thymidine residues adjacent to a 22 bp duplex that contained thymidine at every other position. Surprisingly, the KMnO₄ reactivity pattern extended from the ssDNA into the dsDNA region of the substrate. Lengthening the partial duplex to 30 bp revealed a similar pattern extending from the ssDNA into the dsDNA, indicating that NS3 binds within the duplex region. Increasing the length of the ssDNA portion of the partial duplex by 4 nt resulted in a shift in the footprinting pattern for the ssDNA by 4 nt which is consistent with preferential binding to the 3'-end of the ssDNA. However, the footprinting pattern in the dsDNA region was shifted by only 1–2 bp, indicating that binding to the ss/dsDNA region was preferred. Footprinting performed as a function of time indicated that NS3 binds to the ssDNA rapidly, followed by slower binding to the duplex. Hence, multiple molecules of NS3 can bind along a ss/ds DNA partial duplex by interacting with the ssDNA as well as the duplex DNA.

Keywords

helicase; unwinding; DNA footprinting; KMnO₄

Helicases are molecular motor proteins that use ATP hydrolysis to manipulate nucleic acids (1–4). Helicases disrupt nucleic acid structure as well as remodel protein-nucleic acid complexes. The role of helicases in virtually all nucleic acid metabolic events has lead to in-depth investigations into the mechanism(s) of these enzymes (5). One of the most studied helicases is NS3 from the Hepatitis C virus (HCV) (6–8). The helicase activity of NS3 is required for replication of the HCV genome based on studies using a subgenomic replicon that encodes the HCV nonstructural proteins (9). However, the specific role in HCV viral multiplication played by this enzyme has not been delineated. HCV infection causes chronic liver disease and hepatocellular carcinoma, so understanding the specific role and

*corresponding author: Tel.: (501) 686-5244; fax: (501) 686-8169; raneykevind@uams.edu.

§Current address: Department of Psychiatry, University of Arkansas for Medical Sciences.

\$Current address: Department of Pathology, University of Arkansas for Medical Sciences.

Supporting Information Available. Control experiments are shown as supplemental figure 1 in which the lack of DNA melting was confirmed after prolonged incubation of NS3 with DNA in the absence of ATP. This material is available free of charge via the Internet at <http://pubs.acs.org>.

mechanism of NS3 has significant medical importance. The extensive study of NS3 has made this enzyme a model system for understanding the detailed biochemical mechanism for how helicases manipulate nucleic acids.

Helicases are categorized into several superfamilies based on sequence comparisons (10;11). NS3 is in superfamily 2, which shares basic structural elements with superfamily 1 helicases including the Walker A and Walker B regions that participate in binding and hydrolysis of ATP. NS3 is further classified as a DExH motor protein. The helicase motifs are located within two RecA-like domains forming a cleft in which ATP binding and hydrolysis occurs (12). The two domains are known to move closer together upon binding ATP and then separate after ATP hydrolysis (13;14). The movement of these domains coordinates specific amino acid interactions with the nucleic acid that leads to directionally-biased movement along the RNA or DNA strand (15;16).

Many helicases exhibit a preference for nucleic acid substrate, operating on DNA or RNA, but not necessarily both. Although RNA is believed to be the biological substrate for NS3, this enzyme also functions equally well on DNA in vitro (9;17). Presently, there is no known biological role for NS3 functioning on DNA, although the protein has been found in the nuclei of patients infected by HCV (18;19). Characterization of the DNA binding and unwinding activities of NS3 has significance for our overall understanding of how this model system selects specific nucleic acid structures. Previous studies suggest that NS3 interacts with the nucleic acid substrate at a single-stranded/double-stranded (ss/ds) junction (20), but structural characterization of this interaction is lacking.

Biophysical and kinetic experiments indicate that NS3 can interact with itself *in vitro* and that oligomers (17) or dimers (21) are responsible for optimal unwinding of short DNA or RNA substrates, respectively. A monomeric form is also capable of unwinding DNA (22) and RNA (23). Previous work suggested that the DNA substrate was coated by NS3 molecules under conditions in which optimal DNA unwinding was observed (17). Multiple molecules of NS3 or the helicase domain (NS3h) have been proposed to line up along the ssDNA portion of a partial duplex substrate and function together to enhance DNA unwinding activity (24). This phenomenon has been referred to as functional cooperativity. In this report, the spatial orientation and number of NS3 molecules bound to ssDNA and partial-duplex substrates has been investigated by DNA footprinting using KMnO₄. Results indicate that binding energy of the enzyme pre-disposes the duplex DNA for melting. A model is proposed whereby multiple molecules of NS3 bind to the DNA substrate and participate in the binding and unwinding process.

Materials and Methods

DNA oligonucleotides were from Integrated DNA Technologies (Coralville, Iowa) and purified by preparative gel electrophoresis. [γ -³²P]ATP was purchased from PerkinElmer Life Sciences. T4 polynucleotide kinase was obtained from New England Biolabs. HEPES, BME, SDS, MOPS, Tris, NaCl, Na₄EDTA, BSA, acrylamide, bis-acrylamide, MgCl₂, KOH, ATP, formamide, xylene cyanole, bromophenol blue, urea, KMnO₄, and glycerol and MgCl₂ were purchased from Fisher. Streptavidin dynabeads were from Invitrogen.

Recombinant full-length NS3 was derived from the HCV Con 1b replicon consensus sequence. NS3 was expressed as a fusion protein with a sumoylation tag (SUMO) on the N-terminus. Protein purification was performed by initially capturing expressed protein on a nickel affinity column via a (His)₆ tag on the N-terminus of the SUMO fusion. The SUMO fusion protein was cleaved by incubation with Ulp 1 protease, followed by a second round

of nickel affinity chromatography. Final polishing of NS3 was performed by heparin sepharose and anion exchange chromatography as described (17).

DNA footprinting with KMnO₄

DNA footprinting reactions were modified from a procedure established by Bui *et al.*, 2003 (25). DNA oligonucleotide substrates were designed with a biotin label located adjacent to the 5'-end. A nucleotide was placed at the 5' end for radiolabeling with ³²P. Footprinting reactions were performed at 37° C in buffer consisting of 25 mM MOPS, pH 7.0, 50 mM NaCl, 10 mM MgCl₂, and 0.2 mg/mL BSA. Aqueous KMnO₄ (100 mM) was stored frozen at -80° C and thawed immediately prior to use. Radiolabeled DNA substrates (10 nM) in buffer were incubated with NS3 (concentrations listed in figure legends) for 9 min at 37° C followed by addition of KMnO₄ up to a final concentration of 3.3 mM. The footprinting reaction proceeded for 5 s followed by quenching upon addition of 1 M sME and 200 mM EDTA. Dynabeads M-280 Streptavidin (0.04 mg/ml) were added to the solution and vortexed at room temperature for 30 min. DNA-bound Dynabeads were captured by magnetic isolation, suspended in a solution (100 NL) containing 1 M piperidine and 0.1 mM biotin, and heated to 90° C for 30 min. Dynabeads were removed and the solution was evaporated using a SpeedVac. The dried residue was dissolved in 30 μL of H₂O and re-evaporated twice to remove residual piperidine. The DNA samples were suspended in denaturing buffer (95% formamide, 0.025% SDS, 0.025% SDS, 0.025% xylene cyanole, 0.025% bromophenol blue) and separated by electrophoresis on a denaturing 20% polyacrylamide gel. The DNA bands were quantified by using a Typhoon PhosphorImager and ImageQuant software (GE Healthcare, Piscataway, NJ). The footprinting data were analyzed by determining the radioactivity in each band corrected for background in triplicate experiments. The sum total radioactivity in each lane was determined and the fraction of the total in each individual band was calculated. The fraction of radioactivity for each band in the presence of NS3 was divided by the fraction in the absence of NS3 to obtain "thymidine reactivity" which represents the relative reactivity of each thymidine position with permanganate in the presence *vs.* the absence of NS3.

Results

NS3 binding to ssDNA results in a repeating pattern of high reactivity and protection towards KMnO₄

NS3 binding to DNA has been determined for various forms of the enzyme. Most quantitative binding data have been obtained using only the helicase domain (NS3h). NS3h binding to ssDNA (12mer) has resulted in a K_D value of 10 nM whereas binding to a duplex resulted in a K_d value of 1 NM (20). Additional experiments support specific binding of NS3h to a ss/dsDNA junction or a 'fork' structure (20). However, NS3h is not directly comparable to NS3, because the presence of the protease domain changes the affinity for nucleic acid. The full-length NS3 has been examined for binding using fluorescence anisotropy and electrophoretic mobility shift assays (EMSA). The K_D value for binding to a 15mer ssDNA was 4.7 nM whereas binding to a blunt end duplex of 30 bp resulted in a K_D value of 16 nM (17). Hence, NS3 behaves quite differently than NS3h in binding to duplex DNA. It should be noted that different genotypes of NS3 behave differently in binding and activity assays, so direct comparisons between studies must take into account not only the form of the enzyme (NS3h vs. NS3), but also the specific genotype (26). Furthermore, NS3 activity is modulated by a cofactor, NS4A, which can stimulate unwinding activity (27;28), further complicating any direct comparison of binding studies.

Like most helicases, NS3 requires a ssDNA overhang to rapidly initiate unwinding of DNA. The length of the ssDNA overhang can be varied to accommodate more than one molecule

of NS3, resulting in increased unwinding, as was shown for the NS3 helicase domain (24). NS3 is known to bind to ssDNA with a site-size of 8 nt (29) which is consistent with the reported co-crystal structures (12–14). DNA unwinding experiments are often conducted in the presence of an enzyme concentration that exceeds the substrate concentration. The number of NS3 molecules bound to a specific DNA substrate prior to initiation of a DNA unwinding experiment can be estimated based on the binding site-size and the length of the ssDNA. We wished to directly measure the number of molecules of NS3 bound to a specific DNA substrate, so a DNA footprinting assay was applied using KMnO₄ which can react with thymidine residues at the C-5 and C-6 carbon positions (25;30). After reaction with KMnO₄, treatment of the DNA with piperidine results in a cascade of reactions leading to cleavage of the DNA backbone, which can be visualized after separating different sized DNA fragments by gel electrophoresis. Thymidine residues that are exposed, such as in ssDNA, are highly reactive, whereas residues in dsDNA are much less reactive because the site of reaction is sterically shielded. Additionally, protein binding might sequester thymidine residues, which may alter reactivity, depending on whether the C5-C6 carbons are facing the protein or the solvent.

NS3 was incubated with a biotin-labeled oligonucleotide made up of 23 thymidines, a biotin-labeled spacer, and a 5'-guanine followed by treatment with KMnO₄ (Fig. 1). In the absence of NS3, uniform reactivity was observed for all of the thymidine residues (Fig. 1A). In the presence of NS3, the polyacrylamide gel revealed a distinct pattern of protection and reactivity. The residues at the 3'-end were reactive, however positions 3, 4 and 5 were protected. The bases at positions 7 and 8 exhibited a high level of reactivity. A second region of protection was followed by another region of reactivity at positions 15 and 16. The results were quantified by determining the amount of radioactivity in each band and dividing it by the sum total of radioactivity in the lane to determine the fraction of DNA in each band. The fraction of radioactivity in each band in the presence of NS3 was divided by the fraction of radioactivity in the corresponding band in the absence of NS3 to determine the relative reactivity of each thymidine towards KMnO₄. The average of three independent values was plotted for each thymidine position (Fig. 1B). The resulting graph indicates that three molecules of NS3 are bound to the oligonucleotide (Fig. 1B, inset), which is consistent with the binding site size for NS3 of 7–8 nt based on the crystal structures of NS3 helicase domain in the presence of ssDNA (12). The fact that the crystal structure of NS3 indicates 5–6 nucleotides in the binding site, whereas the pattern of reactivity repeats every 7–8 nt suggests that the NS3 molecules are packed closely together on the ssDNA. The sites of high reactivity appear to be located between adjacent NS3 molecules as depicted in the inset model showing NS3 bound to the ssDNA.

NS3 binds to the ssDNA and dsDNA regions of a partial duplex DNA substrate

DNA unwinding experiments are typically performed using substrates containing a ssDNA overhang. Binding of NS3 to a DNA substrate containing a 3'-overhang has been proposed to result in melting of a few base pairs in the duplex (20). We examined this possibility using the footprinting reaction, which can report on melted regions of DNA. A partial duplex DNA substrate was prepared containing thymidine residues at each position in the ssDNA region and at every other position in the dsDNA (Fig. 2). Treatment of the DNA alone with KMnO₄ resulted in a clear pattern of high reactivity in the ssDNA region but little reactivity in the dsDNA region as expected (Fig. 2A). Incubation of the DNA (10 nM) with NS3 (500 nM) followed by treatment with KMnO₄ lead to a distinct pattern of reactivity in the ssDNA region that was similar to that observed in figure 1; a peak of reactivity at position 8, flanked by two regions of protection (Fig. 2B). Reactivity increases near the ss/dsDNA junction at position 15, indicating that two molecules of NS3 are bound to the ssDNA portion of the substrate. This result provides direct evidence that under

conditions of excess enzyme concentration relative to DNA, more than one molecule of NS3 is positioned on a 15 nt DNA substrate.

Interestingly, the thymidine residues in the duplex portion of the substrate exhibited much higher reactivity towards KMnO₄ in the presence of NS3 than in its absence (Fig. 2A). Radioactivity in these bands was quantified and the reactivity for each position was plotted (Fig. 2C; positions are designated by the letter “d” for duplex). The relative reactivity of thymidines in the duplex region increases much more than the ssDNA regions because the reactivity in the absence of NS3 is very low. The pattern of reactivity and protection was strikingly similar to that observed in the ssDNA. Two regions of high reactivity centered on positions 8d and 16d were flanked by regions of lower reactivity. Further, the pattern of protection and reactivity in the duplex was an extension of the pattern that started on the single-stranded DNA, with regions of high reactivity being separated by approximately 7–8 nucleotides beginning at the 3'-end.

The reactivity was examined using a DNA substrate that was the same length as in Figure 2, but the thymidine residues were placed into the displaced strand, rather than the tracking strand (Fig. 3A). The thymidine reactivity was plotted for the duplex region by numbering each position from the ss/dsDNA junction. The pattern of reactivity matched closely to that shown for the tracking strand, with peaks of reactivity at position 8d and 16d (Fig. 3B).

The appearance of a footprinting pattern in the duplex region led us to examine a longer duplex substrate containing 30 bp. The ssDNA overhang exhibited the familiar pattern as the other substrates (Fig. 4), and the duplex region exhibited a strong footprinting pattern, especially near the ss/dsDNA junction (Fig. 4B). The highest thymidine reactivity within the duplex occurred at position 8d, which is 8 bp from the ss/dsDNA junction. This result suggests that at least one molecule of NS3 is bound within the duplex region. The pattern of reactivity continues within the duplex, exhibiting additional reactivity peaks at position 16d and position 24d. Hence, the reactivity pattern repeats every 8 bp.

It is possible that NS3 melts the duplex by sequestering ssDNA formed due to thermal fraying. However, control experiments in the absence of ATP indicated that only 3% of the 22 bp substrate was separated during a ten minute incubation time (Supplemental Figure 1). No melting was observed in control experiments with the 30 bp substrate (not shown). Therefore the increased reactivity of the duplex region towards KMnO₄ is not due to complete separation of the duplex upon NS3 binding. Rather, the increased reactivity is likely due to partial melting that leads to greater accessibility of the KMnO₄ for the C5 and C6 atoms of thymidine residues in the duplex region. NS3 appears to be capable of binding to the dsDNA and readily capturing the ssDNA at the junction.

NS3 binding to blunt-ended dsDNA

A blunt-ended 30mer duplex was prepared (Table 1) and examined for binding by KMnO₄ footprinting (Fig. 5A). The reactivity pattern indicated some binding to the duplex, perhaps due to fraying at the ends (Fig. 5B). Hence, NS3 is readily capable of capturing DNA at the ends of the duplex as depicted in the diagram in Figure 5C. Reactivity within the interior of the blunt-ended duplex was less evident compared to the substrates that contained a ssDNA overhang.

Increasing the length of the ssDNA overhang shifts the pattern of reactivity in the ssDNA

The thymidine reactivity exhibited a repeating pattern of ~8bp pattern, consistent with the site-size of NS3. In order to further examine the pattern of reactivity, a partial duplex substrate was prepared in which the ssDNA overhang was increased in length by 4 nt from 15nt to 19nt. The duplex region remained the same at 22bp with a thymidine residue

occupying every other position (Table 1). KMnO₄ footprinting resulted in a peak of reactivity at positions 7 and 8 in the ssDNA region (Fig. 6A), similar to that which was observed with the 15nt substrate (Fig. 1B and Fig. 2B). A minor peak of reactivity in the 19nt ssDNA was observed at position 15, but was not clearly defined. Hence, the reactivity pattern in the ssDNA was shifted by 4 nt, consistent with NS3 binding to the 3'-end of the ssDNA.

The reactivity pattern in the duplex region exhibited a peak at position 6d (Fig. 6B). This peak is shifted compared with the peak of reactivity observed for the 15nt:22bp substrate (Fig. 2B) or the 15nt:30bp substrate (Fig. 4B) which occurred at position 8d. The resolution of the reactivity pattern is limited to 2bp, so the shift in the peak is 1–2 bp in the duplex region compared to the other substrates. In contrast, the initial reactivity pattern of the ssDNA region of the 19nt:22bp substrate is similar to that of the 15nt:22, exhibiting a shift of 4 nt. The reactivity pattern in the remainder of the ssDNA is less well defined (Fig. 6A). The reactivity pattern in the duplex region of the 19nt:22bp substrate is similar to that observed for the other dsDNA regions. The fact that the pattern in the duplex region exhibits only a small shift in the position of the reactivity peak supports the conclusion that NS3 prefers to bind to the ss/dsDNA junction.

NS3 binds to the ssDNA rapidly, then more slowly binds to the dsDNA region

Binding of NS3 to the single-stranded and duplex regions of the substrate was examined by probing with KMnO₄ as a function of increasing incubation times. The gel image clearly indicates that the ssDNA region is bound very rapidly because the protection pattern appears in the first 30 s (Fig. 7A). However, the increased reactivity in the duplex appears more slowly. The reactivity of the DNA towards KMnO₄ was determined as described above and plotted for thymidine residues in the ssDNA region (Fig. 7B) or in the dsDNA region (Fig. 7C) as a function of incubation time. The reactivity in the ssDNA region exhibits little or no change during the 9 min incubation time. However, the reactivity in the duplex region increases, as is shown for selected thymidine positions in Figure 7C. The increase in reactivity is especially noted at thymidine residues in the interior duplex region such as positions 8d and 16d. The increase in reactivity is a measure of the increased propensity for KMnO₄ to react with thymidine residues. The reactivity of KMnO₄ within the duplex region of the DNA does not reflect complete strand separation, but instead must reflect a transition in the local structure of the duplex DNA that leads to greater reactivity of thymidine with KMnO₄. We conclude that the dsDNA is partially melted or untwisted to some degree, thereby exposing the reactive sites of thymidine to KMnO₄.

NS3 binds the duplex region even at relatively low concentrations relative to the DNA substrate

Binding of NS3 to the 15nt:22bp substrate was investigated by varying the enzyme concentration. NS3 (50, 100, 250, 500, or 1000 nM) was incubated for 9 minutes with DNA (10 nM) followed by reaction with KMnO₄ for 5 s. Each DNA molecule contains five binding sites for NS3 based on a 7–8 nt binding site size so that 10 nM substrate can bind 50 nM NS3 (two sites in the ssDNA region and three possible sites in the duplex region). Comparison of the reactivity in the ssDNA region (Fig. 8A) with the reactivity in the dsDNA region (Fig. 8B) indicates that the pattern of protection and reactivity appears within the duplex region of the substrate even at the lowest concentration of NS3 (see expanded view in Fig. 8C). The reactivity peak is not clearly observed at the lowest concentration of NS3 for the ssDNA region (Fig. 8A). This may be due to random binding of NS3 to ssDNA at low concentration of NS3 which might result in general protection of the ssDNA. However, the pattern of protection is observed in the dsDNA region, which further supports a preference for binding to the ss/dsDNA junction. Hence, multiple molecules of NS3 bind

along the DNA, even when the concentration of NS3 is similar to the concentration of available binding sites. This result also supports the conclusion that the majority of the enzyme is available for binding to the DNA, as previously reported (17;31).

Discussion

In describing the mechanism of helicases, it is useful to distinguish between translocation on ssDNA and melting of duplex DNA. The two processes are clearly related, and may indeed occur in the same step in the overall mechanism for DNA unwinding for some helicases. However, there are mechanisms in which translocation and melting are distinguishable, and different experimental methods can report on different aspects of the mechanism. The reported structures of NS3 clearly illustrate the path of the ssDNA through the active site in the enzyme (12–14). ATP binding causes closure of the two RecA domains, which is coupled to directionally-biased movement through the ‘ratchet-like’ interactions between amino acid residues such as the base stacking interaction between Trp501 and ssDNA. Translocation on ssDNA or ssRNA is believed to occur in 1 nt steps per each ATP molecule hydrolyzed, although coupling efficiency varies between specific forms of the enzyme (16;27).

The number of base pairs that can be melted for each translocation step is under active debate. A 9 bp RNA substrate was designed that could be melted by NS3 in a single sub-step, as indicated by the lack of a lag phase and the 90% amplitude observed during single-cycle unwinding (32). Although the RNA duplex contained 9 bp, some of the bp may melt spontaneously due to thermal fraying, so the specific number of bp melted in a single-cycle is difficult to reveal in an ensemble experiment. Single molecule Forster resonance energy transfer (smFRET) (33) and structural studies (13) have suggested a “spring-like” motion whereby domains 1 and 2 move by 1 nt increments while domain 3 engages the nucleic acid more tightly through interaction with amino acid residue Trp501. The relative movement of the domains is proposed to build up strain which is released after 3 translocation steps leading to unzipping of three base pairs. An alternative explanation for melting was provided by studies in which single molecule laser tweezers were used to measure step sizes of 0.5 to 3 bp (34). The explanation provided for the variable melting step was based on a proposed second site on the surface of NS3 for binding to the displaced strand. Translocation of NS3 on the tracking strand by 1 nt steps was proposed, but release of the displaced strand was suggested to occur in a manner that does not correlate precisely with translocation, giving rise to the appearance of variable step sizes for bp melting. Identification of the residues responsible for binding to the displaced strand may help delineate the differences in the proposed mechanisms (35).

A Brownian motor mechanism has also been proposed for translocation and unwinding by NS3 helicase domain (NS3h) (20). In this mechanism, two states of binding to DNA, weak and tight, are modulated by ATP binding. In the weak ATP-bound state, NS3h diffuses along the DNA. Hydrolysis and release of the co-factor leads to a tight binding state and directional movement occurs as a result of an asymmetric ‘sawtooth’ energy profile. Based on the ongoing discussion for the mechanism of unwinding by NS3, this area of study will likely remain an active area of investigation and the enzyme will likely continue to serve as a model system for other helicases.

A model for NS3 binding to ss/dsDNA junctions

In this report, we have utilized a method that has the potential to report on the position of the helicase on the DNA as well as the status of the DNA. KMnO₄ reacts with thymidine residues more rapidly than other bases, with the rate of reaction dependent on the exposure of the C5–C6 atoms (i.e. single-stranded vs. double-stranded). This approach has been used

extensively to examine interactions between RNA polymerase holoenzyme and promoters during transcription initiation (36). Some investigators have applied this approach to study helicase binding to DNA (37;38). One study showed a specific role for DNA melting as a result of helicase binding for the RecBCD enzyme. Melting of 6 bp of dsDNA upon binding of RecBCD in the presence of Mg²⁺ allows the enzyme to overcome a kinetic barrier to begin rapid unwinding of DNA (38).

Experiments in this report were designed to determine the number and position of NS3 molecules bound to a DNA substrate prior to initiation of an unwinding reaction. The number of molecules bound to the ssDNA substrate clearly correlated directly to the binding site-size of the enzyme, which is 7–8 nt. Surprisingly, NS3 was found to interact with the duplex portion of the substrate, producing a reactivity pattern with KMnO₄ that extended the pattern observed on ssDNA. Binding to the ssDNA occurs very rapidly (less than 15s), whereas binding to the duplex occurs more slowly, but within the first five minutes of incubation under conditions used here (Fig. 7). This result indicates that interaction of NS3 with dsDNA leads to partial melting of the duplex which exposes some thymidine residues for reaction with KMnO₄. Alternatively, NS3 is poised to capture ssDNA due to thermal fraying, perhaps as a result of a preferential interaction at the ss/dsDNA junction. These results are consistent with a previous report indicating that NS3 binds relatively well to dsDNA (K_D value between 10–20 nM) (17). The results also suggest that multiple molecules of NS3 are poised to participate in the unwinding reaction when NS3 concentration is in excess of DNA substrate concentration. A model for the interaction between NS3 and the 15nt:22bp substrate is shown in Fig. 9. Initial binding occurs with two NS3 molecules along the ssDNA region. Additional molecules of NS3 then bind more slowly to the dsDNA adjacent to those already bound to the ssDNA. Binding of NS3 to the duplex may pre-dispose the DNA for melting in the presence of ATP. Binding of dsDNA does not lead to complete separation of the duplex initially, but instead causes some degree of untwisting, or partial melting, which increases reactivity of thymidine residues with KMnO₄.

Previous work indicated that unwinding by NS3 was highly sensitive to the structure of the duplex (39). Structural alteration of the displaced strand led to slower unwinding, suggesting that NS3 interacts with the displaced strand. More recent reports using single molecule experiments (40) also indicated that NS3 is highly sensitive to the structure of the duplex region of a substrate. The results reported here using DNA footprinting clearly show interaction of NS3 with the duplex region which provides an explanation for why this enzyme is sensitive to the duplex structure. The reactivity of the duplex region with KMnO₄ in the presence of NS3 indicates that the duplex is actively engaged by the enzyme. Under conditions in which the enzyme concentration greatly exceeds the substrate concentration, the interaction between NS3 and duplex DNA may be facilitated by the propensity of NS3 to form oligomeric structures (17;22). In such a mechanism, binding of NS3 to the ssDNA region of a partial duplex substrate could help recruit additional molecules to the duplex region through protein-protein interactions.

One of the important implications of the data here is that the number of molecules of NS3 bound to the substrate is not defined exclusively by the length of the ssDNA overhang. The 15nt ssDNA overhang can clearly bind two molecules of NS3, as shown by the DNA footprinting patterns. NS3 can also bind within the duplex portion; therefore, more molecules of NS3 may be poised to participate in the unwinding reaction than predicted by the length of the ssDNA. Hence, it may not be possible to limit the number of molecules bound to the substrate by simply varying the length of the ssDNA. Additionally, the number of bp melted during the unwinding reaction may also be difficult to discern because some bp appear to be melted simply due to binding.

NS3 exhibits a very large kinetic step size of ~16 bp in ensemble experiments (17;21) and 11 bp in single molecule experiments (34;40). Mechanisms proposed to account for the large kinetic step size include fast unwinding followed by a slower step that limits the overall appearance of ssDNA. The slow step has recently been proposed to be due to binding of both DNA strands to NS3, with slow release of the displaced strand limiting the rate of processive unwinding (35). It is possible that the physical basis for large kinetic step size does not correlate with the rapid unzipping observed in single molecule experiments. The results from DNA footprinting favor an interaction between NS3 and both strands of the substrate, producing a protein-DNA complex that untwists or partially melts a relatively large region of the dsDNA prior to initiation of ATP-dependent strand separation. If untwisting or partial melting of the dsDNA is necessary for the subsequent unwinding reaction to ensue, then this process may limit the overall rate of unwinding, thereby providing the slow step in the overall kinetic mechanism.

Whether NS3 binding to DNA has a biological impact on HCV infection remains to be determined. NS3 can affect activities in the nucleus through its interaction with p53 (19), ATM (41), and SRCAP (42), all known regulators of gene expression. However, such protein-protein interactions can occur outside the nucleus thereby altering localization of nuclear proteins, which can lead to changes in DNA metabolism. NS3 has been detected in the nuclei of patients infected with HCV, but DNA binding *in vivo* has not been shown explicitly (18). Regardless of the biological outcomes of NS3 with DNA, understanding the similarities and differences by which NS3 interacts with DNA and RNA is mechanistically valuable, because it is not known exactly how helicases distinguish between the two biological polymers.

Supplementary Material

Refer to Web version on PubMed Central for supplementary material.

Acknowledgments

We thank Alicia K. Byrd for helpful discussions and comments on the manuscript.

Funding Source Statement: This work was supported by NIH grant GM089001 (K.D.R. and C.E.C.), NIH Grant #P20 RR-16460 (L. Cornett) from the IDeA Networks of Biomedical Research Excellence (INBRE) Program, and NIH Award Number UL1RR029884 (C. Lowery) from the NCATS.

Abbreviations used

dsDNA	double-stranded DNA
ssDNA	single-stranded DNA
NA	nucleic acid
NS3	non-structural protein 3
HCV	hepatitis C virus
SF	superfamily
KMnO₄	potassium permanganate
smFRET	single molecule Förster resonance energy transfer

References

1. Lohman TM, Tomko EJ, Wu CG. Non-hexameric DNA helicases and translocases: mechanisms and regulation. *Nat. Rev. Mol. Cell Biol.* 2008; 9:391–401. [PubMed: 18414490]
2. Patel SS, Donmez I. Mechanisms of helicases. *J. Biol. Chem.* 2006; 281:18265–18268. [PubMed: 16670085]
3. Pyle AM. Translocation and unwinding mechanisms of RNA and DNA helicases. *Annu. Rev. Biophys.* 2008; 37:317–336. [PubMed: 18573084]
4. Singleton MR, Dillingham MS, Wigley DB. Structure and mechanism of helicases and nucleic acid translocases. *Annu. Rev. Biochem.* 2007; 76:23–50. [PubMed: 17506634]
5. Myong S, Ha T. Stepwise translocation of nucleic acid motors. *Curr. Opin. Struct. Biol.* 2010; 20:121–127. [PubMed: 20061135]
6. Frick DN. The hepatitis C virus NS3 protein: a model RNA helicase and potential drug target. *Curr. Issues Mol. Biol.* 2007; 9:1–20. [PubMed: 17263143]
7. Morikawa K, Lange CM, Gouttenoire J, Meylan E, Brass V, Penin F, Moradpour D. Nonstructural protein 3-4A: the Swiss army knife of hepatitis C virus. *J. Viral Hepat.* 2011; 18:305–315. [PubMed: 21470343]
8. Raney KD, Sharma SD, Moustafa IM, Cameron CE. Hepatitis C virus non-structural protein 3 (HCV NS3): a multifunctional antiviral target. *J. Biol. Chem.* 2010; 285:22725–22731. [PubMed: 20457607]
9. Lam AM, Rypma RS, Frick DN. Enhanced nucleic acid binding to ATP-bound hepatitis C virus NS3 helicase at low pH activates RNA unwinding. *Nucleic Acids Res.* 2004; 32:4060–4070. [PubMed: 15289579]
10. Fairman-Williams ME, Guenther UP, Jankowsky E. SF1 and SF2 helicases: family matters. *Curr. Opin. Struct. Biol.* 2010; 20:313–324. [PubMed: 20456941]
11. Gorbalenya AE, Koonin EV. Helicases: amino acid sequence comparisons and structure-function relationships. *Curr. Opin. Struct. Biol.* 1993; 3:419–429.
12. Kim JL, Morgenstern KA, Griffith JP, Dwyer MD, Thomson JA, Murcko MA, Lin C, Caron PR. Hepatitis C virus NS3 RNA helicase domain with a bound oligonucleotide: the crystal structure provides insights into the mode of unwinding. *Structure.* 1998; 6:89–100. [PubMed: 9493270]
13. Appleby TC, Anderson R, Fedorova O, Pyle AM, Wang R, Liu X, Brendza KM, Somoza JR. Visualizing ATP-Dependent RNA Translocation by the NS3 Helicase from HCV. *J. Mol. Biol.* 2011; 405:1139–1153. [PubMed: 21145896]
14. Gu M, Rice CM. Three conformational snapshots of the hepatitis C virus NS3 helicase reveal a ratchet translocation mechanism. *Proc. Natl. Acad. Sci. U.S.A.* 2010; 107:521–528. [PubMed: 20080715]
15. Matlock DL, Yeruva L, Byrd AK, Mackintosh SG, Langston C, Brown C, Cameron CE, Fischer CJ, Raney KD. Investigation of translocation, DNA unwinding, and protein displacement by NS3h, the helicase domain from the hepatitis C virus helicase. *Biochemistry.* 2010; 49:2097–2109. [PubMed: 20108974]
16. Rajagopal V, Gurjar M, Levin MK, Patel SS. The Protease Domain Increases the Translocation Stepping Efficiency of the Hepatitis C Virus NS3-4A Helicase. *J. Biol. Chem.* 2010; 285:17821–17832. [PubMed: 20363755]
17. Tackett AJ, Chen Y, Cameron CE, Raney KD. Multiple full-length NS3 molecules are required for optimal unwinding of oligonucleotide DNA in vitro. *J. Biol. Chem.* 2005; 280:10797–10806. [PubMed: 15634684]
18. Errington W, Wardell AD, McDonald S, Goldin RD, McGarvey MJ. Subcellular localisation of NS3 in HCV-infected hepatocytes. *J. Med. Virol.* 1999; 59:456–462. [PubMed: 10534726]
19. Muramatsu S, Ishido S, Fujita T, Itoh M, Hotta H. Nuclear localization of the NS3 protein of hepatitis C virus and factors affecting the localization. *J. Virol.* 1997; 71:4954–4961. [PubMed: 9188558]
20. Levin MK, Gurjar M, Patel SS. A Brownian motor mechanism of translocation and strand separation by hepatitis C virus helicase. *Nat. Struct. Mol. Biol.* 2005; 12:429–435. [PubMed: 15806107]

21. Serebrov V, Pyle AM. Periodic cycles of RNA unwinding and pausing by hepatitis C virus NS3 helicase. *Nature*. 2004; 430:476–480. [PubMed: 15269774]
22. Sikora B, Chen Y, Lichti CF, Harrison MK, Jennings TA, Tang Y, Tackett AJ, Jordan JB, Sakon J, Cameron CE, Raney KD. Hepatitis C virus NS3 helicase forms oligomeric structures that exhibit optimal DNA unwinding activity in vitro. *J. Biol. Chem.* 2008; 283:11516–11525. [PubMed: 18283103]
23. Ding SC, Kohlway AS, Pyle AM. Unmasking the active helicase conformation of nonstructural protein 3 from hepatitis C virus. *J. Virol.* 2011; 85:4343–4353. [PubMed: 21325413]
24. Levin MK, Wang YH, Patel SS. The functional interaction of the hepatitis C virus helicase molecules is responsible for unwinding processivity. *J. Biol. Chem.* 2004; 279:26005–26012. [PubMed: 15087464]
25. Bui CT, Rees K, Cotton RG. Permanganate oxidation reactions of DNA: perspective in biological studies. *Nucleosides Nucleotides Nucleic Acids*. 2003; 22:1835–1855. [PubMed: 14533885]
26. Lam AM, Keeney D, Eckert PQ, Frick DN. Hepatitis C virus NS3 ATPases/helicases from different genotypes exhibit variations in enzymatic properties. *J. Virol.* 2003; 77:3950–3961. [PubMed: 12634355]
27. Beran RK, Lindenbach BD, Pyle AM. The NS4A protein of hepatitis C virus promotes RNA-coupled ATP hydrolysis by the NS3 helicase. *J. Virol.* 2009; 83:3268–3275. [PubMed: 19153239]
28. Pang PS, Jankowsky E, Planet PJ, Pyle AM. The hepatitis C viral NS3 protein is a processive DNA helicase with cofactor enhanced RNA unwinding. *EMBO J.* 2002; 21:1168–1176. [PubMed: 11867545]
29. Levin MK, Patel SS. Helicase from hepatitis C virus, energetics of DNA binding. *J. Biol. Chem.* 2002; 277:29377–29385. [PubMed: 12034714]
30. Holstege FC, Timmers HT. Analysis of open complex formation during RNA polymerase II transcription initiation using heteroduplex templates and potassium permanganate probing. *Methods*. 1997; 12:203–211. [PubMed: 9237164]
31. Jennings TA, Mackintosh SG, Harrison MK, Sikora D, Sikora B, Dave B, Tackett AJ, Cameron CE, Raney KD. NS3 helicase from the hepatitis C virus can function as a monomer or oligomer depending on enzyme and substrate concentrations. *J. Biol. Chem.* 2009; 284:4806–4814. [PubMed: 19088075]
32. Wang Q, Arnold JJ, Uchida A, Raney KD, Cameron CE. Phosphate release contributes to the rate-limiting step for unwinding by an RNA helicase. *Nucleic Acids Res.* 2010; 38:1312–1324. [PubMed: 19969541]
33. Myong S, Bruno MM, Pyle AM, Ha T. Spring-loaded mechanism of DNA unwinding by hepatitis C virus NS3 helicase. *Science*. 2007; 317:513–516. [PubMed: 17656723]
34. Cheng W, Arunajadai SG, Moffitt JR, Tinoco I Jr, Bustamante C. Single-base pair unwinding and asynchronous RNA release by the hepatitis C virus NS3 helicase. *Science*. 2011; 333:1746–1749. [PubMed: 21940894]
35. Serebrov V, Beran RK, Pyle AM. Establishing a mechanistic basis for the large kinetic steps of the NS3 helicase. *J. Biol. Chem.* 2009; 284:2512–2521. [PubMed: 19010782]
36. Gries TJ, Kontur WS, Capp MW, Saecker RM, Record MT Jr. One-step DNA melting in the RNA polymerase cleft opens the initiation bubble to form an unstable open complex. *Proc. Natl. Acad. Sci. U.S.A.* 2010; 107:10418–10423. [PubMed: 20483995]
37. Farah JA, Smith GR. The RecBCD enzyme initiation complex for DNA unwinding: enzyme positioning and DNA opening. *J. Mol. Biol.* 1997; 272:699–715. [PubMed: 9368652]
38. Wong CJ, Lohman TM. Kinetic control of Mg²⁺-dependent melting of duplex DNA ends by Escherichia coli RecBC. *J. Mol. Biol.* 2008; 378:761–777. [PubMed: 18395743]
39. Tackett AJ, Wei L, Cameron CE, Raney KD. Unwinding of nucleic acids by HCV NS3 helicase is sensitive to the structure of the duplex. *Nucleic Acids Res.* 2001; 29:565–572. [PubMed: 11139627]
40. Cheng W, Dumont S, Tinoco I Jr, Bustamante C. NS3 helicase actively separates RNA strands and senses sequence barriers ahead of the opening fork. *Proc. Natl. Acad. Sci. U.S.A.* 2007; 104:13954–13959. [PubMed: 17709749]

41. Lai CK, Jeng KS, Machida K, Cheng YS, Lai MM. Hepatitis C virus NS3/4A protein interacts with ATM, impairs DNA repair and enhances sensitivity to ionizing radiation. *Virology*. 2008; 370:295–309. [PubMed: 17931678]
42. Iwai A, Takegami T, Shiozaki T, Miyazaki T. Hepatitis C virus NS3 protein can activate the Notch-signaling pathway through binding to a transcription factor, SRCAP. *PLoS One*. 2011; 6:e20718. [PubMed: 21673954]

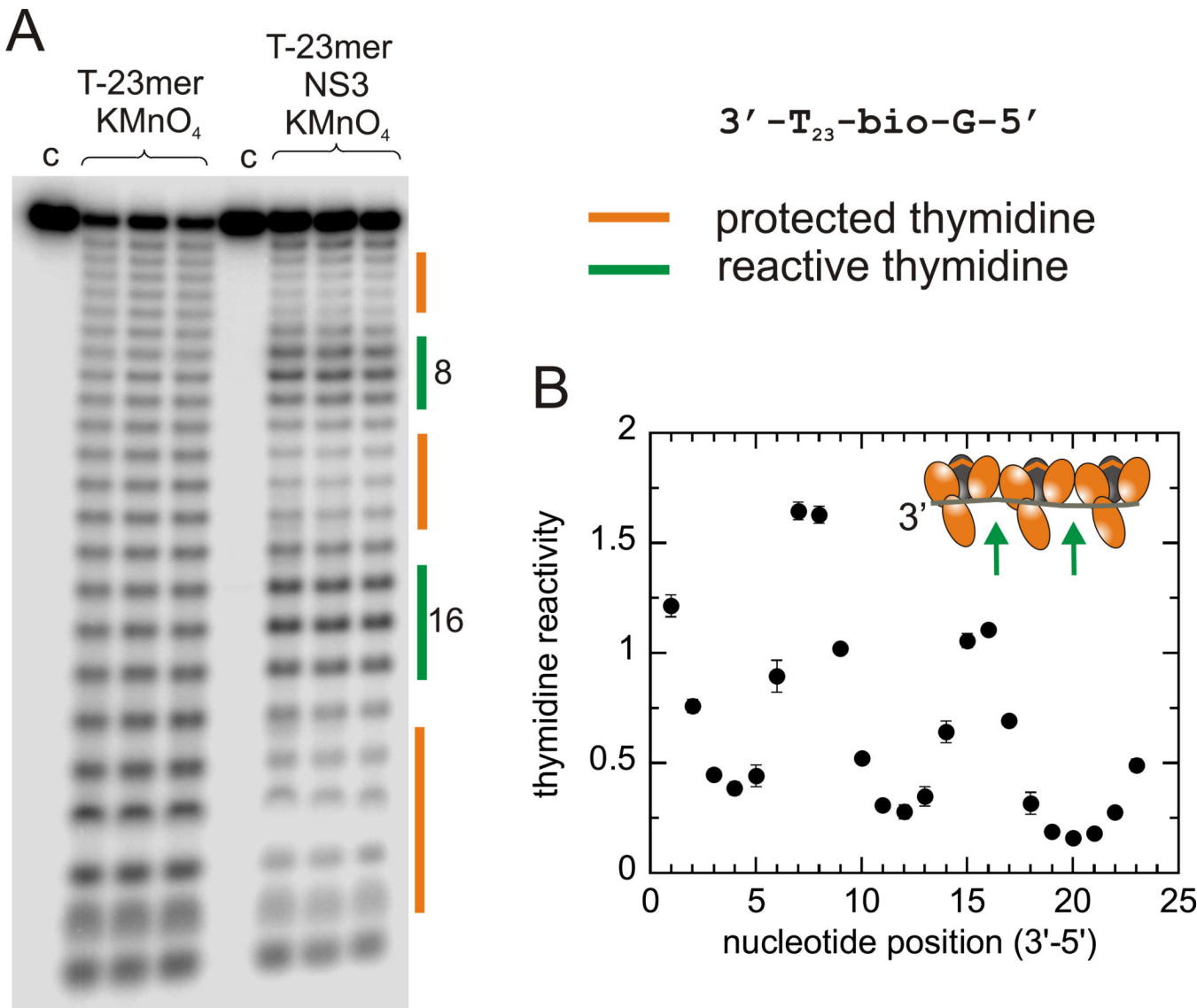


Figure 1. KMnO₄ footprinting reveals binding of NS3 to ssDNA with an 8 nt site-size

A) ssDNA substrate consisting of 23 thymidine residues, a biotin labeled analog, and a 5'-guanine residue was treated with KMnO₄ in the presence or absence of NS3. DNA was isolated on streptavidin beads, treated with piperidine, followed by extensive washing prior to separation on a 20% denaturing polyacrylamide gel. In the presence of NS3, regions of low reactivity and high reactivity were observed as indicated by the orange and green bars. Three regions of protection and two regions of high reactivity are indicated by the orange and green bars, respectively. **B)** Quantitation of the radioactivity in each band in the presence of NS3 was determined and compared to the radioactivity in the absence of NS3 to determine the thymidine reactivity. Each point in the graph is the average of three independent experiments and error bars reflect the standard deviation from the average. The plot revealed two regions of high reactivity separated by 8 nt. A model showing three molecules of NS3 bound to the oligonucleotide is shown in the inset with arrows indicating sites of high thymidine reactivity. Error bars represent the standard deviation from three experiments.

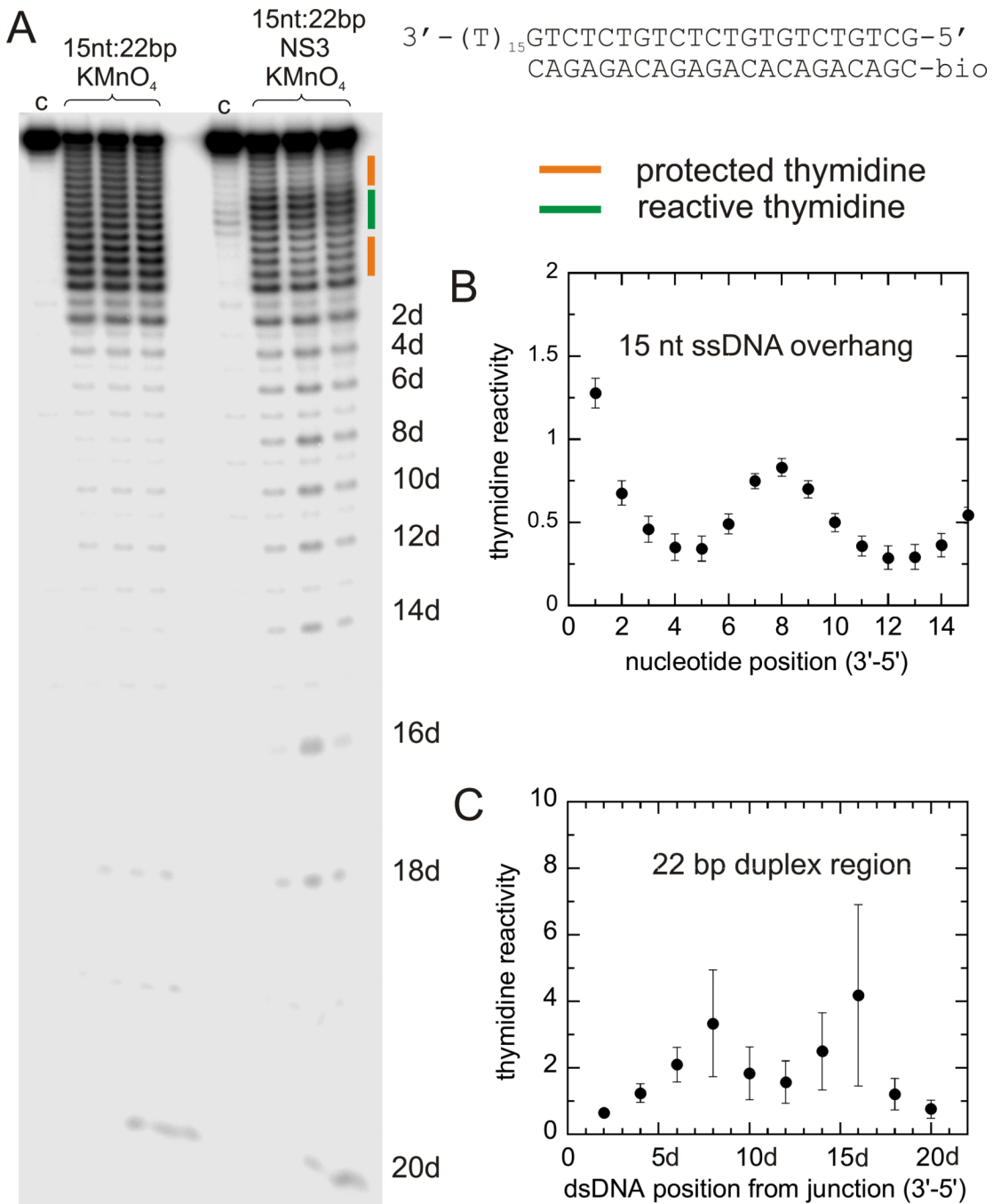


Figure 2. Footprinting with KMnO⁴ reveals NS3 binding to the ssDNA and dsDNA regions of a partial-duplex DNA substrate

A DNA substrate was designed so that each base in the single-stranded region and every other base in the duplex region was thymidine. A complementary 22mer was hybridized to the thymidine strand to produce a 15nt:22bp DNA substrate. **A**) Substrate DNA (10 nM) was incubated in the presence or absence of NS3 (500 nM) for 9 min at 37° C, followed by reaction with KMnO₄. DNA was captured on streptavidin beads followed by treatment with piperidine, and separation on a 20% denaturing polyacrylamide gel. All of the residues in the single-stranded overhang are highly reactive towards KMnO₄. Bands corresponding to the thymidine residues in the duplex region are numbered along the right side of the gel and

generally exhibit much lower reactivity towards KMnO₄. Thymidine residues which are protected or show increased reactivity in the presence of NS3 are indicated by the orange and green bands, respectively. DNA in lanes marked “c” was not treated with KMnO₄. **B)** The thymidine reactivity in the presence of NS3 was divided by the reactivity in the absence of NS3 to determine the effect of NS3 binding on the DNA at each thymidine position. The pattern of reactivity in the ssDNA exhibits a region of high reactivity at position 8 flanked by two regions of protection. **C)** The relative reactivity of each thymidine in the duplex region is plotted. Two regions of high reactivity are observed at positions 23 and 31 indicating that NS3 binds to the entire length of the partial-duplex substrate. Error bars represent the standard deviation from three experiments.

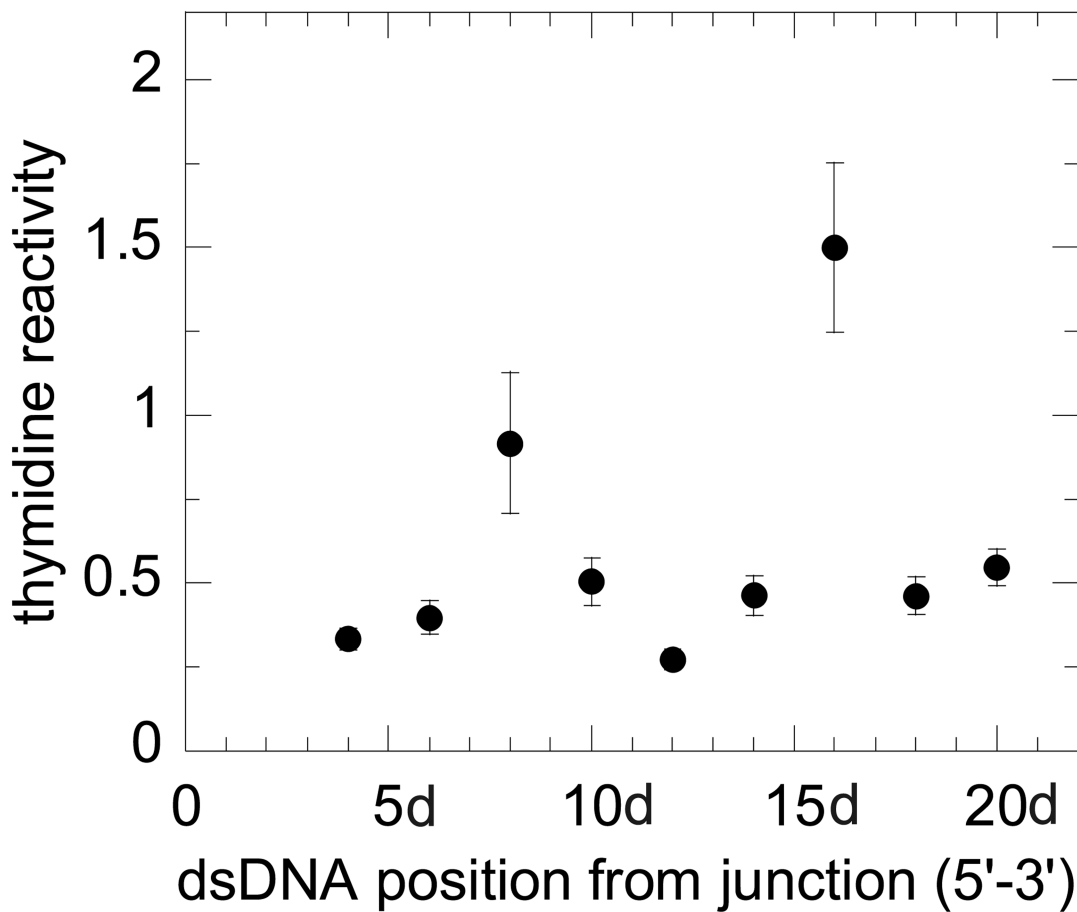
A**B**

Figure 3. Footprinting of the displaced strand provides a similar pattern as the tracking strand
A) A DNA substrate was prepared with 15nt of ssDNA and 22 bp, but the sequence contained thymidine residues at every other position in the displaced strand of the duplex region (15nt:22bpT). **B)** Permanganate footprinting was performed as described and the resulting thymidine reactivity is plotted for the displaced strand. The thymidine residues are numbered from the ss/dsDNA junction (the 5'-end of the displaced strand). The reactivity pattern exhibited peaks at positions 8d and 16d, which corresponds to the reactivity pattern observed for the tracking strand as shown in Figure 2.

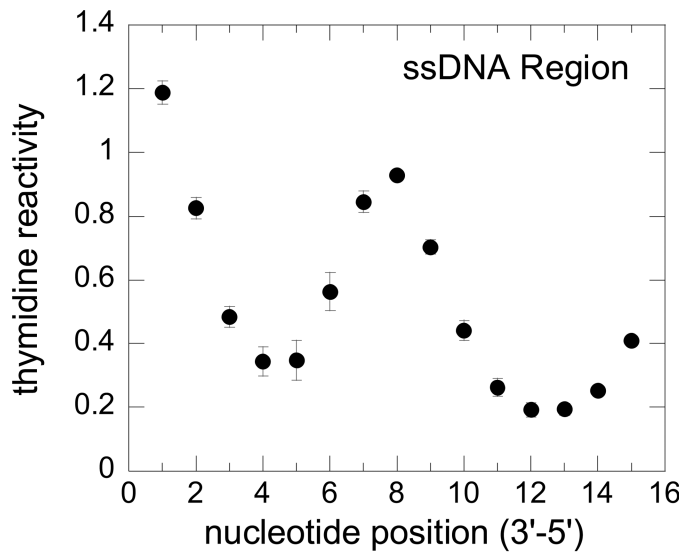
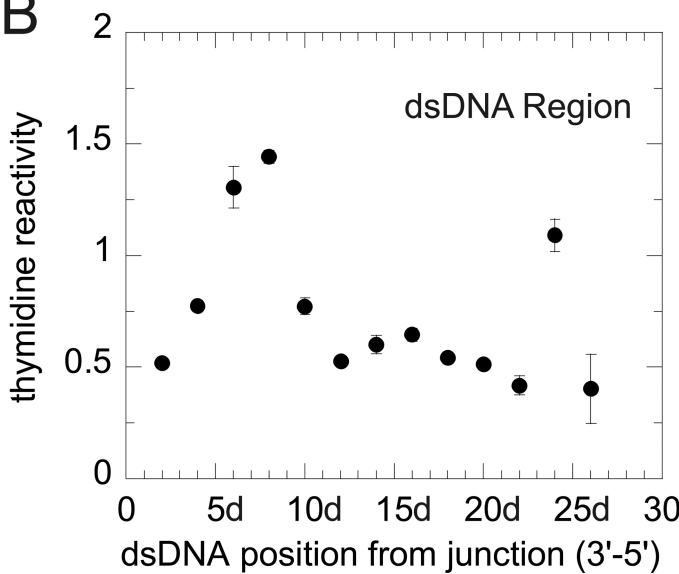
A**B**

Figure 4. KMnO₄ footprinting of NS3 bound to a 15nt:30 bp partial duplex

A) A complementary 30mer was hybridized to the thymidine strand to produce a 15nt:30bp DNA substrate. Substrate DNA (10 nM) was incubated in the presence or absence of NS3 (500 nM) for 9 min at 37° C, followed by reaction with KMnO₄. Thymidine reactivity was determined as described. The pattern of reactivity in the ssDNA region is similar to that observed with the previous substrates, exhibiting a region of high reactivity at position 8 flanked by two regions of protection. **B)** The relative reactivity of each thymidine in the duplex region is shown with positions relative to the ss/dsDNA junction. Three regions of high reactivity are observed at positions 8d, 16d, and 24d indicating that NS3 binds to the

entire length of the partial-duplex substrate. Error bars represent the standard deviation from three experiments.

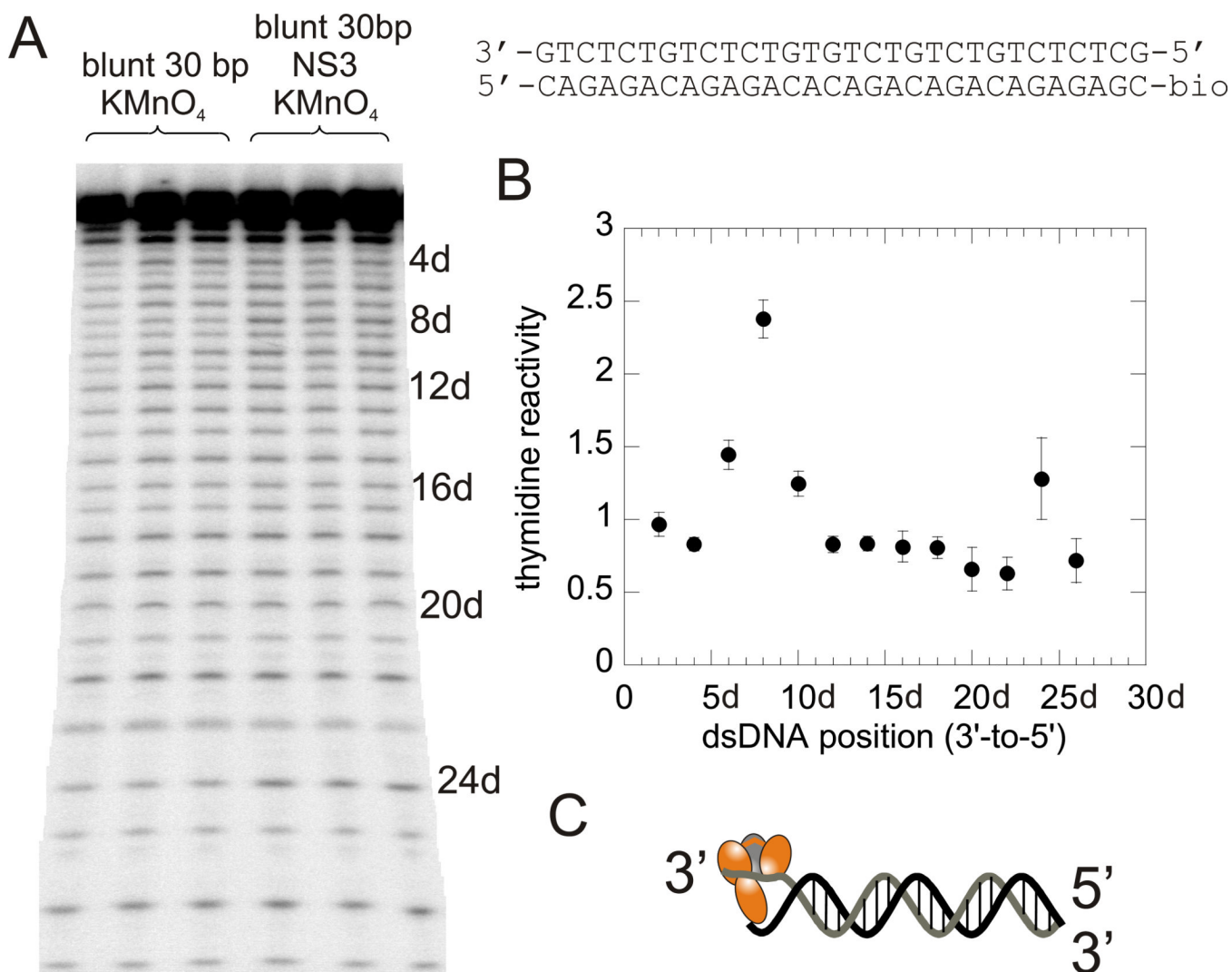


Figure 5. KMnO₄ footprinting reveals NS3 binding to the ends of a blunt-end duplex 30mer
A) A blunt-end 30mer DNA substrate (10 nM) was prepared containing a thymidine residue at every other position in the radiolabeled strand. Permanganate footprinting was performed as described in the absence or presence of NS3 (500 nM). Numbers to the right of the gel indicate the position from the 3'-end of the strand containing thymidine. **B)** Plot of the relative thymidine reactivity in the presence of NS3. The thymidine reactivity pattern exhibited a peak at positions 8d and a minor peak at position 24d. **C)** Model for binding of NS3 to the end of the duplex.

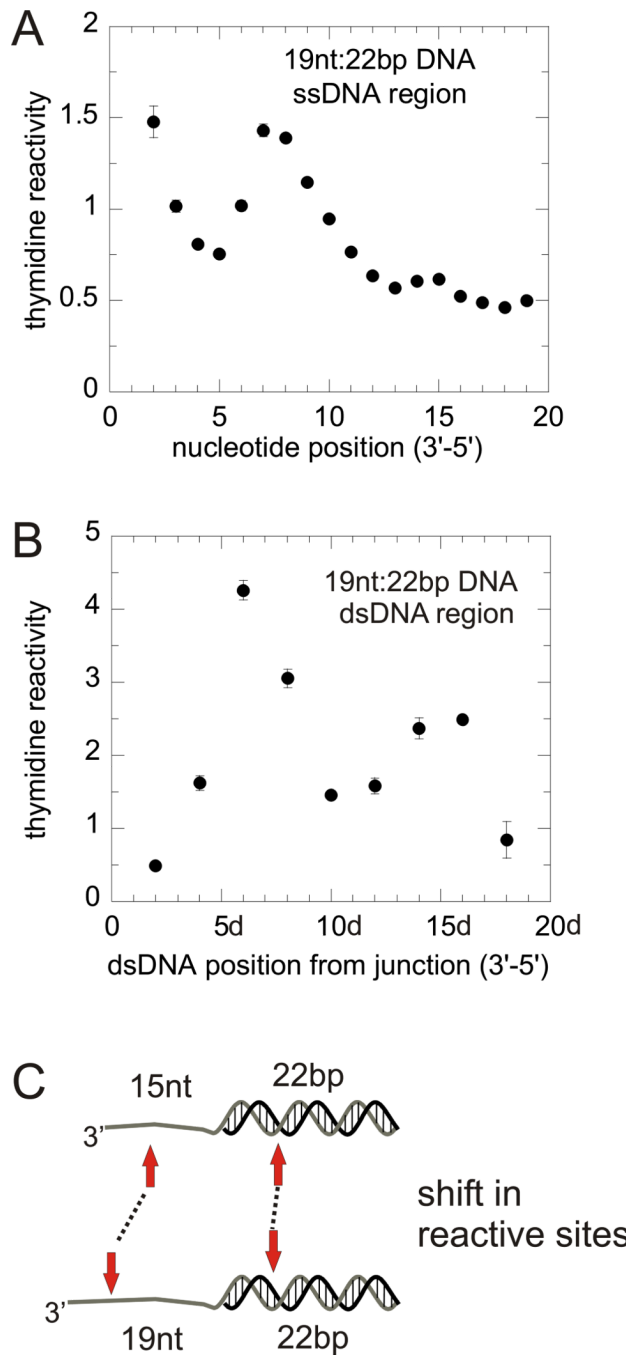
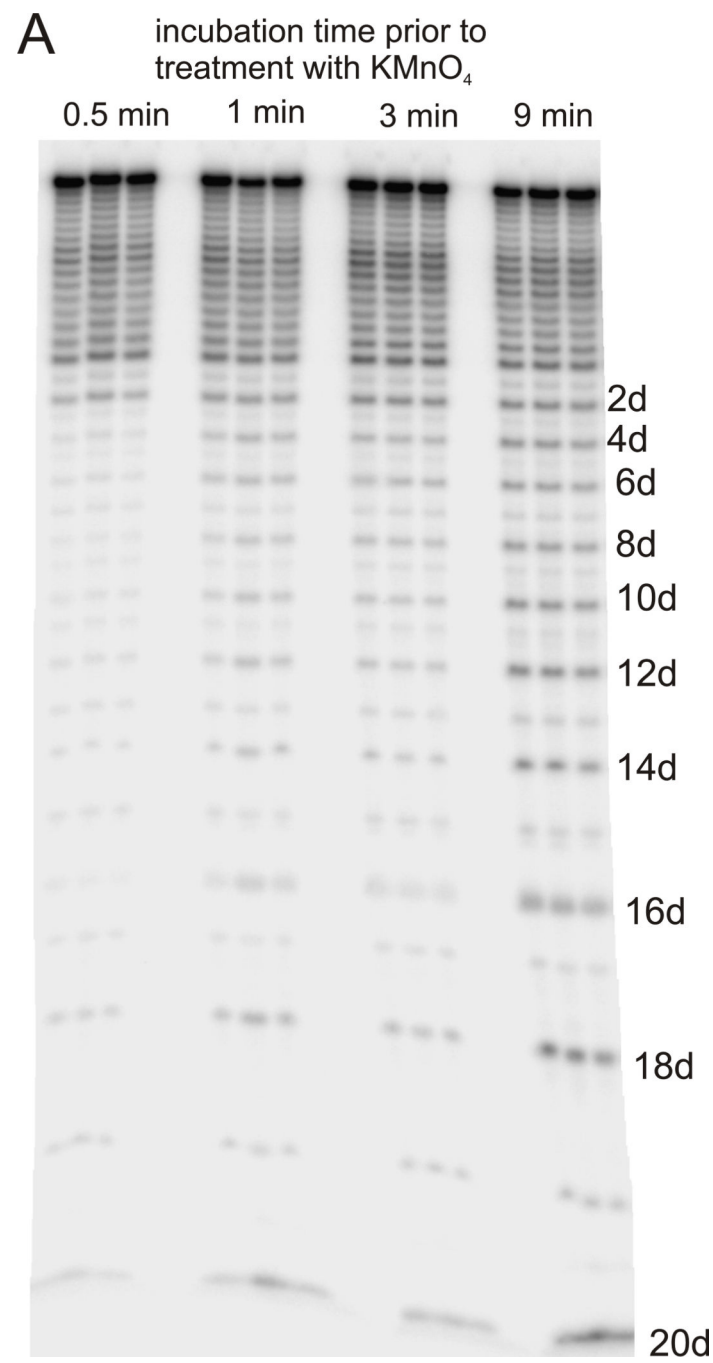


Figure 6. Increasing the length of the ssDNA reveals a shift in the position of KMnO₄ reactivity towards the 3'-end of the ssDNA

A) A substrate was designed such that the ssDNA overhang contained 19 nt and 22 bp. KMnO₄ footprinting was performed in the absence or presence of NS3 (500 nM) as described. The pattern of thymidine reactivity in the ssDNA portion of the substrate exhibited a peak at positions 7–8 and a minor peak at position 15. **B)** The pattern of thymidine reactivity in the duplex region exhibited a peak at position 6d and position 14d. **C)** Diagram showing how the reactive sites for the 15nt:22bp substrate compare to the 19nt:22bp substrate. The major peak in reactivity in the ssDNA region is shifted by 4 nt. The major peak in reactivity in the dsDNA is shifted by 1–2 bp.



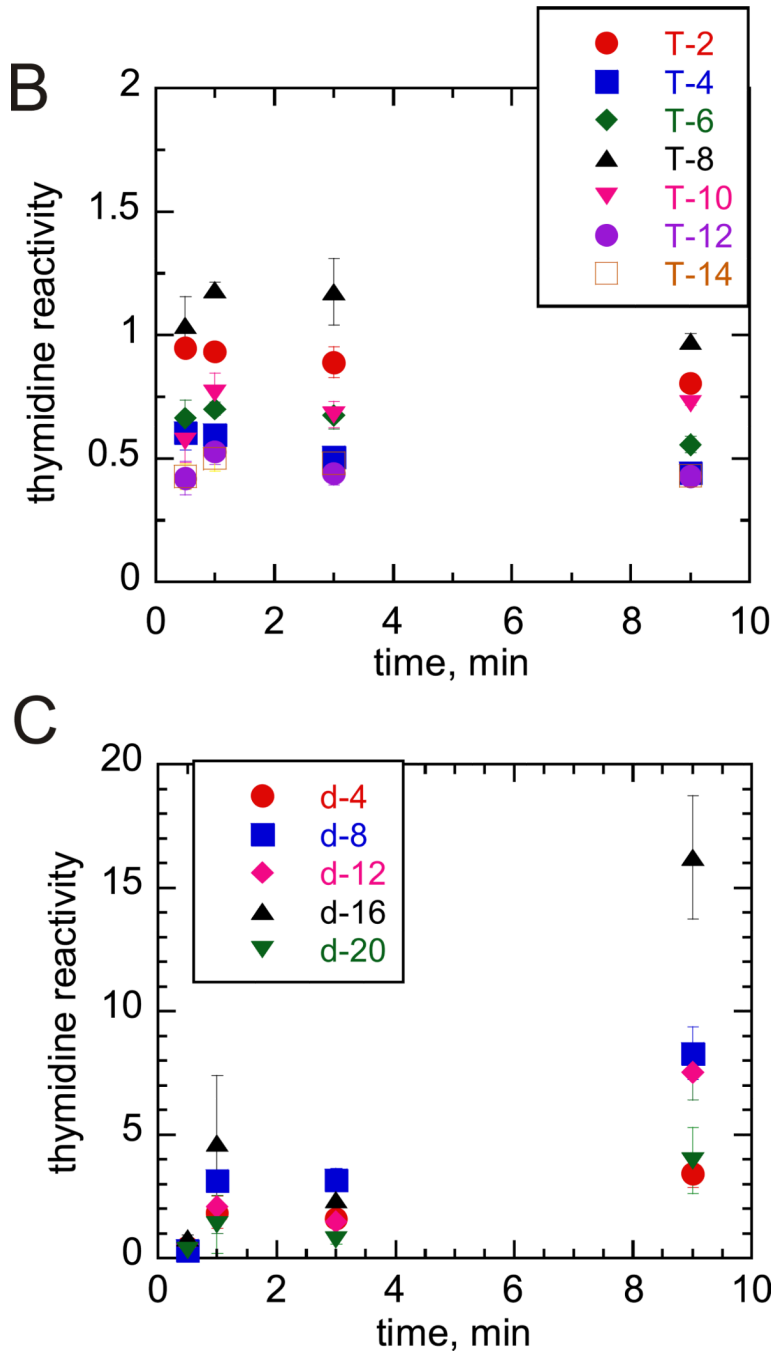


Figure 7. Thymidine reactivity with KMnO_4 determined as a function of incubation time between NS3 and DNA

A) NS3 was incubated with the 15nt:22bp DNA for 0.5, 1.0, 3.0, or 9.0 min at 37 °C, followed by reaction with KMnO_4 for 5 s. DNA was captured on streptavidin beads and treated with piperidine, followed by separation on a 20%, denaturing polyacrylamide gel and visualization using a PhosphorImager. Thymidine positions in the duplex region are numbered to the right of the gel. B) The thymidine reactivity towards KMnO_4 for each band in the ssDNA region was determined as described in “Materials and Methods”. The reactivity was plotted over time and is shown for every other thymidine position in the ssDNA region, as depicted in the legend on the plot. C) The reactivity of thymidine towards

KMnO₄ for selected positions in the dsDNA region is plotted vs. time. The reactivity generally increases as a function of time in the duplex region.

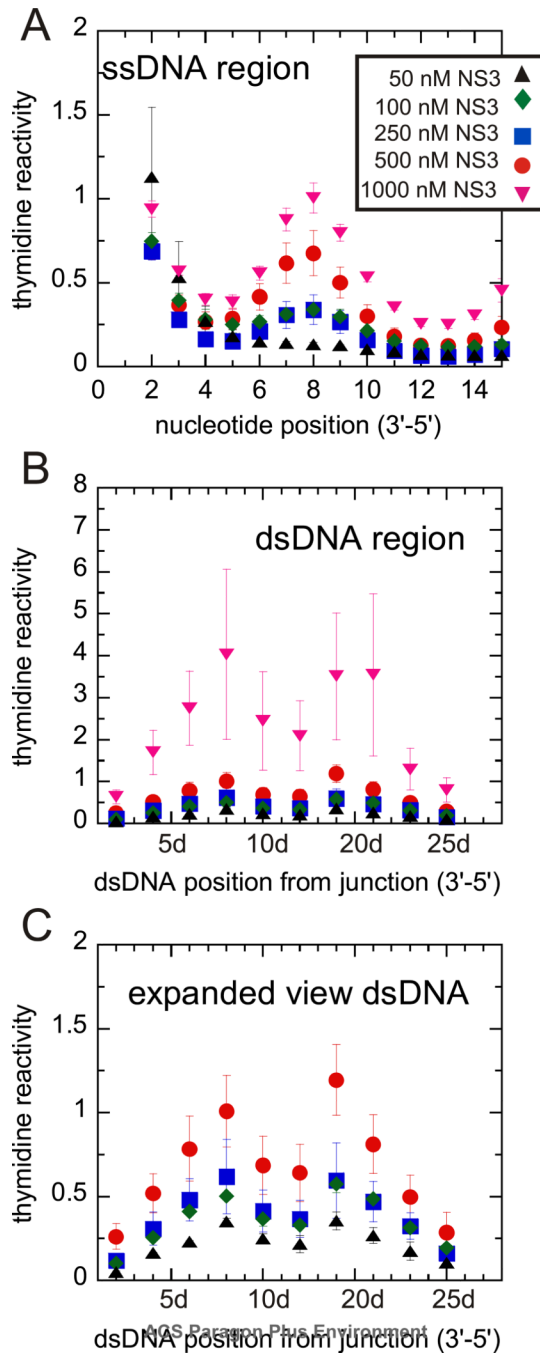


Figure 8. The KMnO₄ footprinting pattern is similar over a range of NS3 concentrations
 Increasing concentrations of NS3, 50 nM (\blacktriangle), 100 nM (\blacklozenge), 250 nm (\blacksquare), 500 nM (\bullet) and 1,000 nM (\blacktriangledown), were incubated with the 15nt:22bp DNA (10 nM) for 9 min followed by footprinting with KMnO₄. Reactivity of thymidine with KMnO₄ is plotted for each position in the ssDNA region (A) or in the dsDNA region (B). C) An expanded view of the dsDNA region. The pattern of protection and reactivity of thymidine with KMnO₄ in the dsDNA region can be observed even at the 50 nM NS3 (black triangles) at which the concentration of available DNA binding sites is equal to the concentration of NS3.

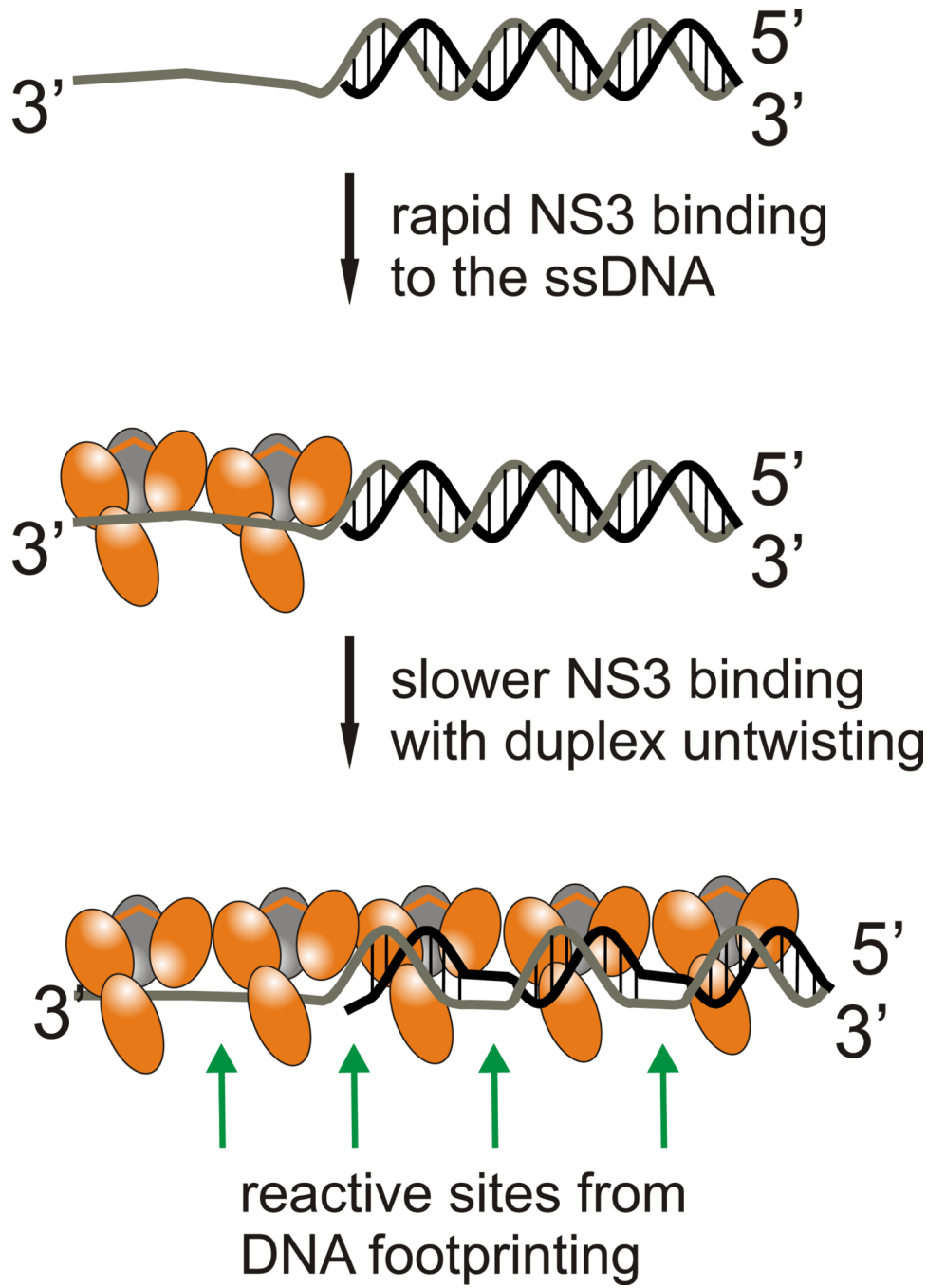


Figure 9. Model for NS3 binding to a partial duplex DNA substrate

Diagram showing NS3 binding to the 15nt:22bp substrate. The model takes into account the data from the DNA footprinting experiments with KMnO₄ which indicate that 7–8 nt (or bp) are bound per NS3 molecule. Initial binding of two molecules of NS3 occurs on the ssDNA overhang, followed by slower binding to the duplex. Binding to the duplex region results in changes in DNA conformation that increase thymidine reactivity with KMnO₄, consistent with untwisting of the duplex.

Table 1

DNA sequences used for KMnO₄ footprinting.

3' (T15)-GTC TCT GTC TCT GTG TCT GTC G-5'	15nt:22bp
5'-CAG AGA CAG AGA CAC AGA CAG C-bio-3'	
3' (T19)-GTC TCT GTC TCT GTG TCT GTC G-5'	19nt:22bp
5'-CAG AGA CAG AGA CAC AGA CAG C-bio-3'	
3'(T15)-GTC TCT GTC TCT GTG TCT GTC TGT CTC TCG-5'	15nt:30bp
5'-CAG AGA CAG AGA CAC AGA CAG ACA GAG AGC-bio-3'	
3'-bio-(T15)-CAG AGA CAG AGA CAC AGA CAG C-5'	15nt:22bpT
5'-GTC TCT GTC TCT GTG TCT GTC G-3'	

The 30mer duplex was derived from the 15nt:30bp sequence by removing the ssDNA.